STAR
Research Journal

Available online at www.starresearchjournal.com (Star International Journal)

PHYSICS

EXPERIMENTAL AND THEORETICAL CHARACTERIZATION OF SILVER OXIDE NANO MATERIAL USING COMPUTATIONAL METHODS

R. VISHNUPRIYA[1] & Dr. M.K. MURALI[2]

[1]*Ph.D Scholar, Department of Physics, J.J. College of Arts and Science,Pudukkottai, Tamilnadu, India.*
[2]*Assistant Professor & Head, Department of Physics, J.J. College of Arts and Science,Pudukkottai, Tamilnadu, India.*

Abstract

The nano metal oxide material; silver oxide (Ag_2O) was prepared in the form of thin film by popular technique; Electron beam evaporation method which was set down on optically flat glass plates. In order to study the structural, morphological and electro-optical properties, the thin film was annealed at 100º, 200º and 300º C temperatures respectively. The FT-IR and FT-Raman spectra were recorded for macro as well as nano levels with different temperatures. The obtained data from SEM, described the amalgamation of nano iso-surface and it was supported by the data attained from TEM. The experimentally observed results and theoretically calculated output were established the silver particle size in the range of 33-50 nm at three different annealed temperatures. The structural parameters and its associated analysis showed the consistent bond length and bond angle parameters. The EDAX deflection peaks displayed the compositional parts of the nano material and it was also figured the presence Ag and O and thereby the sequential array of atoms with lattice was made by Ag_2O combination. The theoretical and experimental data related to UV-Visible absorption spectra revealed the optical data linked with absorption. Its acquired results explained the accurate response of light by the nano Ag_2O and the active visible region was determined. The experimental information regarding Photoluminescence spectrum revealed the semi-optical transparency and opto-electronic effect of the films. The main root-cause of radiative centre of silver oxide nano material was determined and evaluated by the associated outcome results.

Keywords: Ag_2O, EDAX, iso-surface, Photoluminescence, semi-optical transparency.

1. INTRODUCTION

Past some decades, the research on nano-metal particles associated with oxides have great attention due to its multi-dimensional potential applications in the field of opto-electronics, nano electronics and semi-optical material technology [1-3]. Moreover, due to the escalating demand for a wide range of products, goods and attire has endorsed deep study on Ag nano particles fabrication. Among various novel nano-metal oxide nano particles, particularly, the silver (Ag) nano particle materials have been the major nano family of spotlight of the nano scientist since their attractive semi-optical and physico-chemical properties [4-6].

In such a way, these AgO nano particles have prospective usages in various industrial fields, similar to molecular and nano catalysis, nano adopted electronics, bio-active drug, gas-sensing, and in the field of contaminated water treatment [7-8].

Since past decades, the Ag has been used for the human societal development due to its multi-functional applications in optical, mechanical, electronic and pharmaceutical industries. It is also used in ornaments, fashion jewelers, high sensitive photography and architectural industry. Its usage has been extended to the field of pharmaco-industry by their beneficial antibacterial property which is much toxic to fungi, viruses and algae. Silver has extended long been utilized as a disinfectant, such as treating wounds and burns since its wide-spectrum of toxicity to bacteria[9-11].

The growth of new nano metal materials along with oxides (Ag, Au and Cu) and deposition on inert glass materials have increased much consideration in nano-material science since their escalating functions in structural composites of designed optics, medical diagnosis, nano-analytical chemistry and photo catalysis [12-13].

The important argentous metal oxides such as Ag_2O, AgO, Ag_3O_4 and Ag_2O_3 constitute a interesting group which are synthesized in various types of crystal structures which are having variety of motivating physico-chemical properties; bio-electrochemical and electro-optical properties. Hence, the nano silver oxide crystals and thin films were intensively followed for capable applications such as bio and gas sensor for the detection of toxic and fire hazards gases [14-18]. By the optimized nano structures it was also used to fabricate photo conductive and photovoltaic materials which are most significant components in optical memories as well as in Plasmon photonic devices[19-20].

Park et al. [21] have reported the incidence of photoluminescence discharge band in AgO cubic-like structure which was accredited to the localized condition of oxygen vacancies. A weak shoulder peak was identifed at 440 nm due to the bluish green radiation by

the presence of oxygen faults defects in the films. It was also determined that, the luminescence signal shifted to 618 nm ascribed to blue emission due to the oxygen vacancies out of oxygen partial pressure on room temperature. Dallek *et al.* [22] have reported the photo-emissive characteristics of Ag_2O in the blue emission effect which was attributed to the band via band transition.

After screening the previous works on Ag_2O metal oxide nano materials, no work has been found on the theoretical structure prediction of Nano Ag_2O and its important characterization. In this systematic research work, the effective nano Ag_2O thin films were fabricated and annealed at 100º, 200º and 300º C. the prepared materials were characterized experimentally and computationally. The special spectroscopic investigation has been made for knowing the activity of the compositional parts of the materials and the role of components in exposing novel characteristics.

2. EXPERIMENTAL METHODS

The Electron beam evaporation technique is a popular method where in which the electron beam is generated from an accelerated effective electron source in a vacuum condition and to irradiate an evaporate material. It is one of the best vacuum based techniques used for depositing thin films [18-19], which is still extensively used in the nano laboratories and nano electronic industries for depositing metal oxide and particularly metal complex. Thin films of Ag2O were prepared by EB technique using a HINDHI-VAC vacuum unit (model: 12A4D) fitted with electron beam power supply (model: EBG-PS-3K). Well degreased microscopic glass plates have been employed as the substrate.

The instrument is used for prepare the nano material by evaporating and multi-layering metal oxides and metal complexes of different refraction aspects, it is probable to manufacture optical thin films with various multi functional characteristics; anti-reflective thin film, nano filter film and optical film which are able to transmit and refract convinced wide wavelength bands.

The spectroscopically pure Ag_2O powder of 500 mg was blended well bya pestle and mortar. The mixture was hard-pressed and to prepare as pellets by hydraulic pressure method to obtain pellet at the pressure of 500 kg/cm^2 which is used as the base material for making evaporation. The prepared pellet has been taken in a graphite crucible pot and kept in water cooled copper fireside of the embedded electron gun. The regularly pelletized Ag_2O objects were heated in terms of an electron beam subunit from the constant source DC operated filament cathode. The well polished surface of the Ag_2O prepared pellet was interacted by 180º angle deflected electron beam with step up of 5 kV and its operating power density ≈ 2.2 kW/cm^2. The evaporated metal species from Ag_2O pellet were sprayed and deposited as thin films on the optically flat substrates at a pressure of $1X\ 10^{-5}$ m-bar. In this process, each substrate was positioned perpendicular to the line of view at the point of evaporation source at a polar angle to terminate shading effect and also to get optically uniform deposition. The appropriate preparation physical-parameters; source to substrate distance (15 cm) and fractional pressure at 10 to 5 milli bar) were varied and optimized for setting down homogeneous, fine adherent and transparent thin films. The evaporation rate of 0.5 nm/s was used to deposit the complete Ag_2O thin films. In order to examine the consequence of annealing temperature on the structural, optical, electronic and morphological properties, the deposited Ag_2O films have been annealed at 100º, 200º and 300º C respectively.

The structural properties of Ag_2O thin films have been analyzed using PAN analytical X-ray diffractometer with CuKα radiation source with radiation wavelength of 1.5406 Å. The X-ray diffraction (XRD) deflection peaks were recorded in the region 20 - 60 at a scanning speed of $5°\ min^{-1}$. The Morphological studies have been carried out using scanning electron microscopy (SEM) (the usual magnification array from 20X to≈ 30,000X, the spatial resolution region 50 - 100 nm). The bathochromic and hyperchromic UV-Visible absorbance spectra of the Ag_2O thin films have been recorded using a UV-Vis spectrophotometer with different scanning equipment.

3. RESULTS AND DISCUSSION

3.1. MORPHOLOGICAL STUDIES

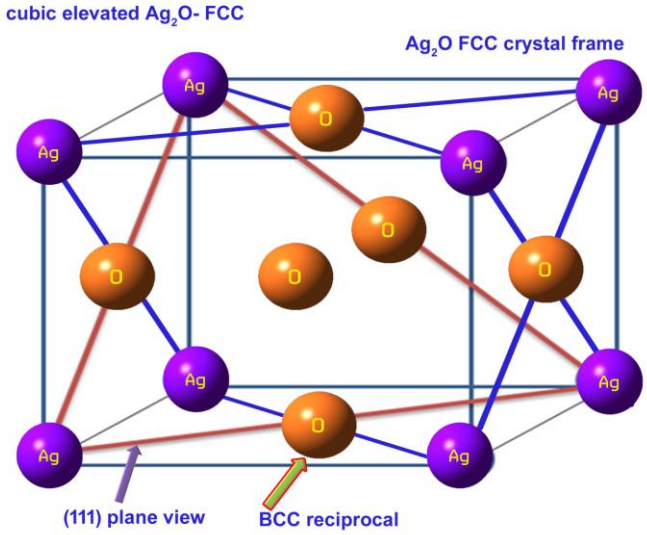

FIGURE 1
CRYSTAL STRUCTURE VIEW OF THE Ag_2O NANO MATERIAL

The crystal structure view of the Ag_2O nano material was presented in the Figure 1 and the atomic placement in the FCC frame was depicted. As per the quantum computational method of calculations, the appropriate single crystal view has been portrayed in which the Ag and O positions were clearly seen. Here, the Ag molecular site with interstitial O appeared to be FCC skeleton whereas the O molecular site along with Ag showed the BCC frame. So that, the FCC crystal frame has definitely having the BCC reciprocal. Three Ag atom from different coordinates connected to form (111) plane where in which the FCC and BCC was validated. According to the figure 1, the O atom was placed the primary corner atom of the BCC lattice whereas the Ag of BCC is the primary corner atom of FCC lattice. Because of this reciprocity, when FCC cuts parallel to optic axis which was to be the perpendicular optic axis of the BCC lattice. When the BCC lattice is engraved perpendicular to the optic axis which is the parallel optic axis of the FCC lattice. Such type of conversion parallel and perpendicular of optic axis of the nano crystal provides second harmonic and tertiary harmonic generation of optical signals.

3.2. SEM EXAMINATION

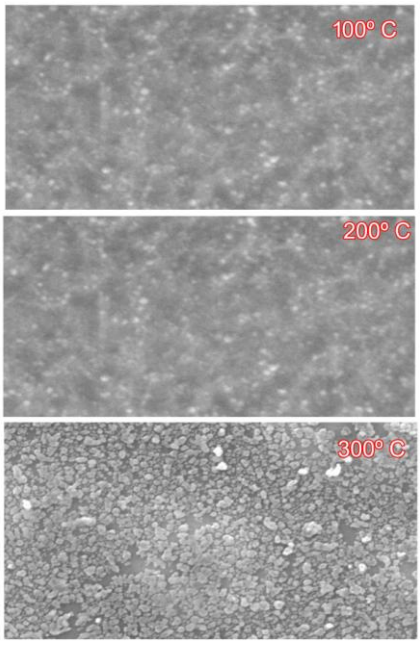

FIGURE 2
SEM SERIES PICTURES

The SEM is a popular tool which is used to display the morphological view of nano and other materials. Due to its high resolution, its results usually compared and validated with the obtained data of TEM. The Scanning electron microscopy technique (SEM) was mainly used for morphological characterization at the nanometre to micrometre scale [23]. The experimentally observed for SEM series pictures were displayed in the Figure 2. In the Figure, the SEM image at 100º C, showed the nano particle amalgamation in which the Ag was perfectly incorporated with O and formed the perfect crystal surface with almost flat character. The SEM figure at 200º C, demonstrated the well defined merged nano surface in which the perfect formation of homogeneous surface was found. The SEM display at 300º C clearly exposed the well arranged discrete nano particle array which was found to be more precious than other two figures. It was also determined that the silver nano particles were globular in form. The amalgamation rate of nano material thin film under study was rapid in annealing temperatures due to the lower melting point of Ag_2O. While come across the previous works [24-26], the SEM of the Ag materials was not able to give any impact on surface whereas the SEM of present case, the iso-surface impression was studied well since the betterment results of SEM.

3.3. TEM Pattern Analysis

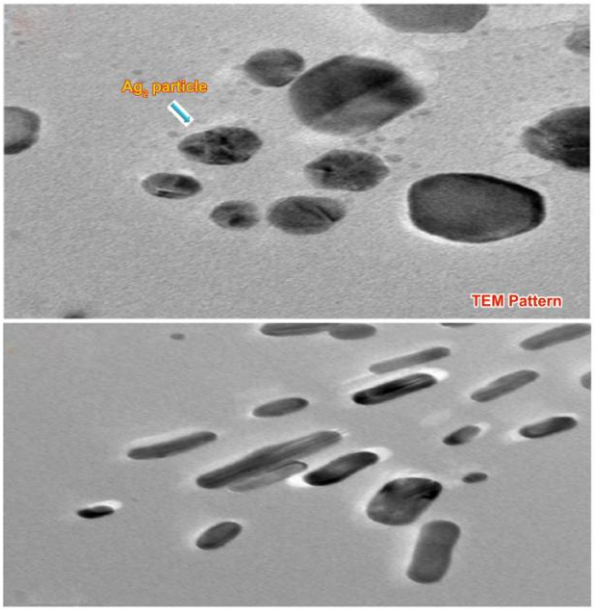

FIGURE 3
TEM IMAGE

The Transmission electron microscope is a popular device which is uses the energetic electron in the champers to study the compositional parts of the material and crystalline information. Usually, the crystal core view and morphological vision can be captured by TEM diagram and making use of it, the nano particle size can be measured accurately. In this case, the TEM image was displayed in the Figure 3 by which the obvious structural morphology and nano particle size of the silver oxide was measured. The instrument is magnified the molecule or crystal in field of view at the maximum potential up to 1 nanometer. TEM is also reproduce two-dimensional images with high-resolution which causes to study the electronic, biological, and different industrial applications [27].

In the TEM figure, the exaggerated image of nano particle; Ag_2O was clearly viewed in which the well defined fringe pattern was observed. The Ag particle in the image was appeared spherical shape with roughed surface. The spherical shape was found to be changed in nearby particles. In addition to that, the nut shaped silver particles were amalgamated in periodic manner with minimum distance of 100 nm. The Particle arrangement was appeared with well defined manner and the particle size was calculated to be 32-51 nm and the calculated particle size was correctly predicted in the XRD computations. The oxygen atom was also appeared over the field of view as the Ag particles and both can be discriminated easily. In the same figure, the well combined nano complex was seen in the form of pellet and the pellets were found to be finely arranged as array. There was no bond impression seen in the field of view since all the atoms in the molecular as well as crystal site were determined to be coordinate covalent bond. The entire particles were associated and were aligned in one direction. From the above observation, it was inferred that, the Ag_2O nano crystal was formed well and the crystallinity was improved when compared with literatures. All the particles were well arranged in the direct FCC lattice and indirect reciprocal site.

3.3. SAED Pattern Analysis

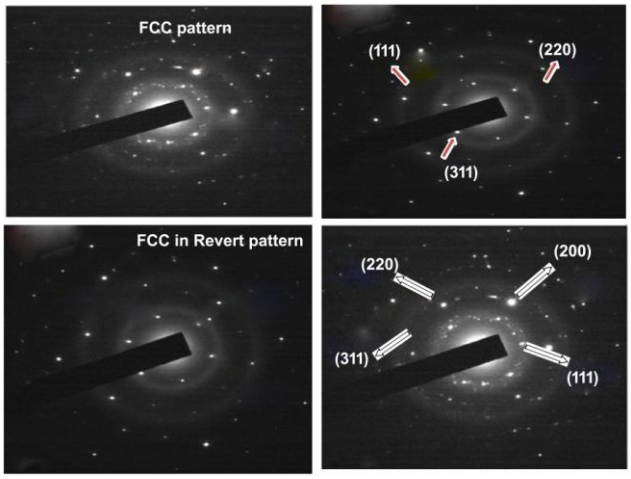

FIGURE 4
SAED SPOT PATTERN OF THE PRESENT NANO METAL COMPLEX

The SEAD technique is generally used for phase identification of fabricated crystal whether in macro or nano level, finding of structural intergrowth due to the interstitial as well as purposive frenkel substitution and evaluating the interplane growth directions. It is also used to trace the kinematically forbidden reflections in the wanted interplane for placing directional atoms [28]. The SAED spot pattern of the present nano metal complex was presented in the Figure 4 in which the FCC lattice pattern was clearly seen.

The selective pattern associated with FCC lattice was recorded and the clear SAED blueprint showed the light spots from (111), (220), (200), (210) and (311) planes. Here, some of the unknown forbidden planes also captured which denoted the reciprocal lattice profile. Hence, the inverted SAED pattern also displayed in the same figure wherein which the hidden reflections from the related planes; (111), (110), (010) and (020) of BCC lattice pattern. Usually, the reciprocal system has not explored by the hidden planes which also explained the normal Lattice. But here, the reverted pattern for BCC lattice also explored upon which the multiple reflections were observed along with adopted normal lattice. This view was supported by the literatures [29-30] and it was confirmed that, the metal complex; Ag_2O nano crystal belongs to FCC lattice.

3.4. EDAX DEFLECTION PATTERN

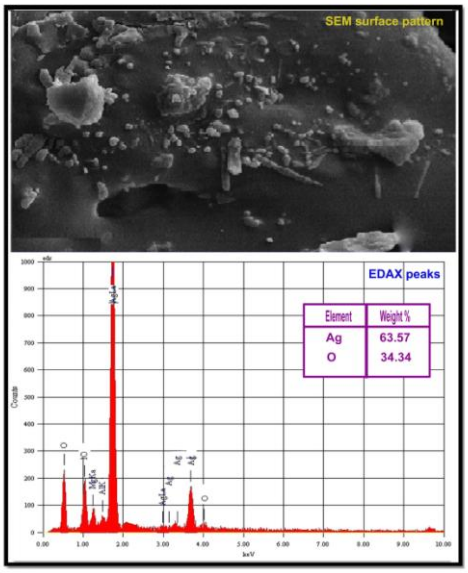

FIGURE 5
DEFLECTION PEAKS WITH FLUCTUATED INTENSITY WITH RESPECT TO THE EXCITATION ENERGY OF THE COMPOSITIONAL PARTS OF THE PRESENT NANO MATERIAL

Normally, the EDAX tools have been used for characterizing the chemical species, functional and non-functional elements in the micro material as well nano materials [31]. The accurate compositional parts of the metal complex and metal oxide composites. The energy associated with present elements can be explored by the application of X-Ray excitation. This analytical techniques usually used for analyze the new materials with different alloys combinations and the strength of the product in material industry. It is also used for troubleshooting and material reformulation for the mechanical and chemical applications [32-33]. The Figure 5 illustrated the deflection peaks with fluctuated intensity with respect to the excitation energy of the compositional parts of the present nano material. From the figure, it was clear that, the transmitted peaks associated with the compositional elements of the present case were appeared in sequential form. The elements were identified according to their weightage and in this case, the Ag and O nano elements were presented with the percentage of 63.57 and 34.34 respectively. The calculated value validated the crystal coordination number of the AgO nano material. The attached figure explored the refined SEM image in which the solidified form of Ag_2O material with smooth surface. The observed elemental peaks of the material absolutely showed the fundamental compositional parts and it also predicted that, the nano material under study, found to be pure and contamination free. From this observation, it was inferred that, the Ag_2O material was having enriched optical and electronic properties. This view was validated by the literatures [34-35].

3.5. UV-Vis SPECTRAL ANALYSIS

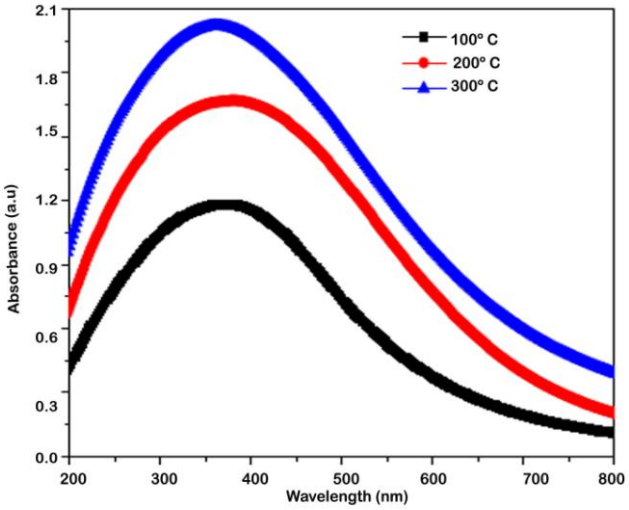

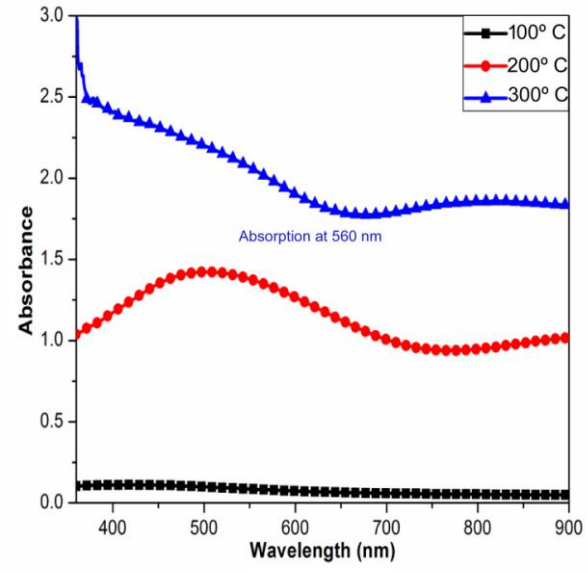

FIGURE 6 & 7
THE PARAMETERS ASSOCIATED WITH THE UV-VISIBLE SPECTRUM

TABLE 1
OPTICAL PARAMETERS OF Ag_2O Thin Films At Different Temperature

Annealing temp in ° C	Refractive index	Band gap (eV)	Extinction coefficient	Absorption Coefficient	Particle size(nm)	ε_1 n^2-k^2	ε_2 2nk
Room temperature	2.233	-	4.6140	0.462×10^{-5}	-	4.221	2.751
100	2.274	1.513	5.237	1.421×10^{-5}	31.52	4.88	2.374
200	2.296	1.545	6.088	0.272×10^{-5}	37.54	4.869	2.804
300	2.323	1.571	6.102	0.241×10^{-5}	42.25	5.016	2.872

Usually, the UV-Visible absorption peaks observed to study the optical response of the nano materials [36]. The UV-Visible absorption measurements in the wide range of wavelength usually used to find the photocatalysis characteristics of the nano materials [37]. The parameters associated with the UV-Visible spectrum were displayed in the Figures 6&7 and the parameters were listed in the Table-1. Here, the characteristics peaks of UV-Visible spectral data were observed at three different annealing temperatures (100º, 200º and 300º C). The peak at 100º has flat absorption which showed no optical response of the material. But, at 200º and 300º C, the signals were found with maximum intensity which clearly demonstrated that, the signal was ranged from 500-560 nm. The observed crest located at exact green region by which it was inferred that, the photo-catalytic character of the Ag nano material was found to be green.

At 300º C, the character was reversed and its corresponding peak was found to be ranged from 400 to 500 nm which explained that, the characteristic wavelength was shifted from green to violet as well as blue regions. So, it was concluded that, the optical response of material was changed with respect to the temperatures and the opto-electronic character of the material can be tuned by the application of temperatures. So the present nano material was having semiconducting property which is able to receive the light and can convert in to photo-excited electronic energy with considerable amount. In addition to that, the present material also has wide range of absorption of visible wavelength with functional temperatures.

From the optical parameters, the optical absorption coefficient was measured and it was in the region from 1.5 to 1.6 eV (photon-energy range) which was supported by the previous works [38-39]. From the direct and indirect optical absorption-transitions in the restricted band gap, the optical absorption coefficient can be analyzed by the equations:

$$\alpha h\gamma = A(h\gamma - Eg)\ m \text{ for } h\gamma > Eg,$$

$$\alpha h\gamma = 0 \text{ for } h\gamma < Eg,$$

The α is the absorption magnitude, A is a band constant, $h\gamma$ - the photon energy, Eg = optical bandgap, m = 2 is an allowed indirect transition and m = 0.5 is an direct transition. The optical band gap was expected by plating the line graph of $(\alpha h\gamma)^{1/2}$ with respect to the photon energy as shown in UV-Visible spectra. The evaluated band gap of the Ag_2O material at 100º to 300º C, were 1.513, 1.545 and 1.571 respectively. The band gap of the material was rather increased with the temperatures and the material has effective optical band gap for generating catalytic action. The observed refractive index for the annealing temperatures from 100º to 300º was 2.274, 2.296 and 2.323 respectively. It was also rather increased according to the temperatures.

3.6. PHOTOLUMINESCENCE OBSERVATION

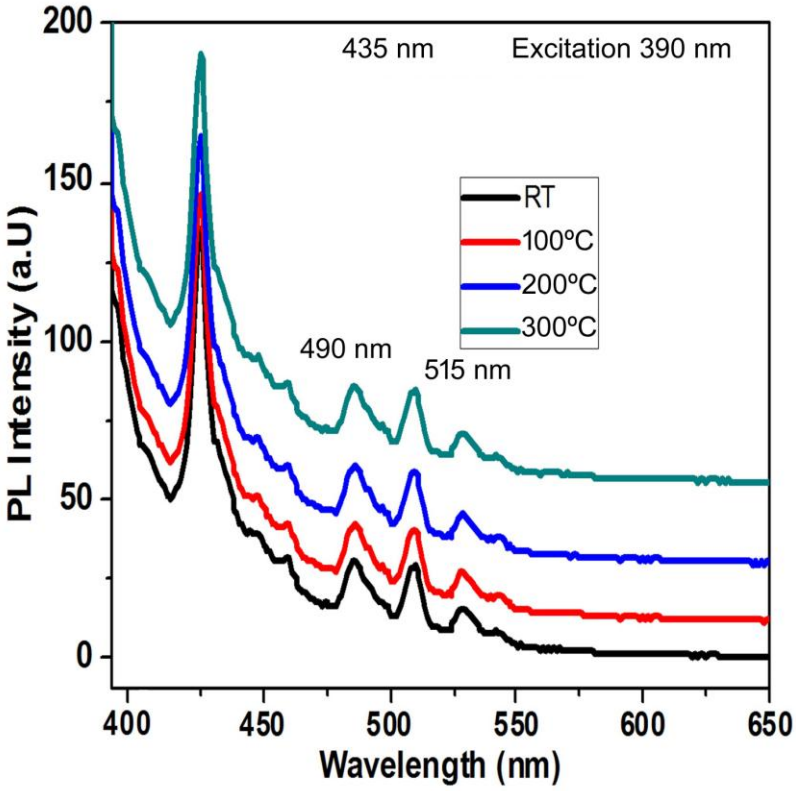

FIGURE 8
PL SPECTRA

The photoluminescence analysis used to characterize the optical and electronic properties of nano semiconductors, nano metal oxides and organic molecules [40]. It is also used to evaluate the metal alloy in-homogeneities and examine the impurity concentration rate of deposition of thin film with different nano metal oxides. The photo-absorption wavelength is not depending upon the nano particle size whereas the PL intensity is found to be inversely proportional to the particle size. The PL absorption due to the electronic excitation always observed well above the Fermi level. In this case the PL spectra was recorded and displayed in the Figure 8. The PL spectra for this case were recorded with different annealing temperatures at the starting excitation wavelength 380 nm in which the signals with different intensity were observed at different wavelengths. The observed emission bands were located at 435, 490, and 515 nm respectively. Among the observed bands, the band at 435 nm was recognized with maximum intensity which was found to be near violet wavelength. Additionally, the attachment of other bands assigned to blue and bluish green wavelengths respectively. From this observation, it was inferred that, the optical characteristics of the present nano Ag_2O material belongs to the visible region and particularly the emission band ranged from violet to blue region. This was purely attributed by the existence of O vacancies which was well agreed with the earlier works [41-42].

From the PL spectra, the refractive index (n) of the nano material was determined using the following relation [36]:

$$R = \frac{(n-1)^2 + K^2}{(n+1)^2 + K^2}$$

Where R is the reflectance value of the Ag_2O thin films

$$\text{Extinction coefficient K} = \frac{\alpha\lambda}{4\pi}$$

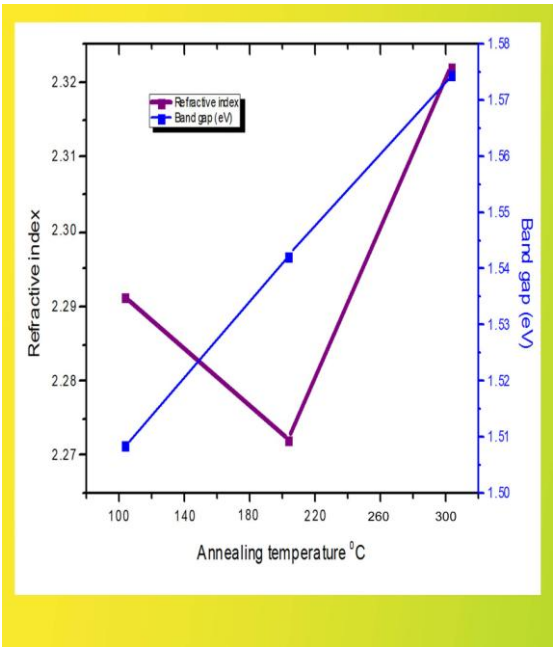

FIGURE 9
THE WAVELENGTH DEPENDENCE OF REFRACTIVE INDEX OF Ag_2O NANO MATERIAL

Here, the n and K were the refractive index and extinction coefficient respectively. The Figure 9 showed the wavelength dependence of refractive index of Ag_2O nano material which was calculated at constant oxygen pressure. From the figure, it was seen that, the refractive index values were found to be decreased with the increment of wavelength for all materials. In addition to that, the observed refractive indices were ranged from 2.2 to 2.3 with annealing temperature.

4.5.3 VIBRATIONAL ANALYSIS

The activeness of the compositional parts of the material whether it is in macro or nano level can be directly evaluated using the FT-IR and FT-Raman spectral pattern. Usually, the atomic basis arrangements are coupled with crystal lattice which is assembled like array in different planes. Each and every plane is having separate bonding of atoms which reflect the radiation falling upon it. The active direct and interplanes of the crystal usually identified from the diffraction peaks from which the lattice frame of the crystal is recognized. Apart from that, using vibrational pattern of the IR and Raman spectra, the active bondings in different planes can be identified and recognized and whichever the planes active for particular lattice type.

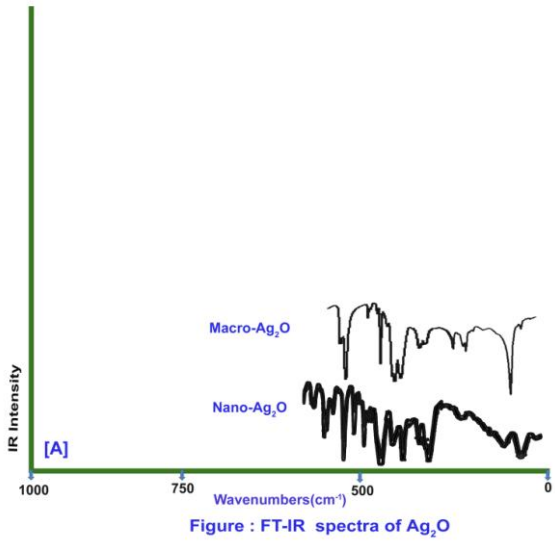

FIGURE 10
FT-IR SPECTRA OF Ag2O

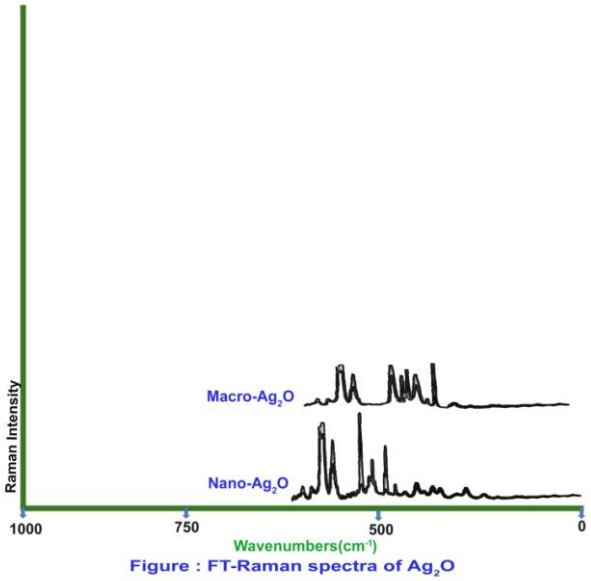

FIGURE 1I
FT-RAMAN SPECTRA OF Ag2O

Here, the FT-IR and FT-Raman spectral pattern were recorded and the assignments associated with the compositional parts can provide the information regarding the vibrationally active bonds and thereby related active planes can be identified. Here, both the spectra in macro as well as nano level of Ag_2O material were depicted in the Table-2 and 3 respectively and their spectra were displayed in the Figure 10 & 11 respectively. Each and every plane is having separate chain of Ag and O by which the sequential form of vibrational regions were assigned. Here, in the case of macro level of Ag_2O, the finger print region was observed in which the Ag-O and Ag-Ag stretching vibrational bands were found at 710, 680, 580 & 480 cm^{-1} and 350 & 270 cm^{-1} respectively. Correspondingly, the Ag-O and Ag-Ag in plane bending vibrations determined at 180 & 160 cm^{-1} and 100 cm^{-1} respectively. The related Ag-O and Ag-Ag out of plane bending vibrational modes were appeared at 150 & 120 cm^{-1} and 80 cm^{-1} respectively.

TABLE 2
EXPERIMENTAL WAVE NUMBERS OF Ag_2O IN MACRO LEVEL

S. No.	Observed Frequency(cm^{-1})		Vibrational assignments
	FT-IR	FT-Raman	
1	710s	710s	(Ag-O)υ
2	680m	680m	(Ag-O)υ
3	580m	580s	(Ag-O)υ
4	480s	480w	(Ag-O)υ
5	350m	350w	(Ag-Ag)υ
6	270m	270w	(Ag-Ag)υ
7	180m	180w	(O-Ag-O) δ
8	160w	160w	(O-Ag-O) δ
9	150w	150w	(O-Ag-O) γ
10	120w	120w	(O-Ag-O) γ
11	100w	100w	(Ag-Ag) δ
12	80w	-	(Ag-Ag) γ

vs; very strong, s; strong, m; medium, w; weak, vw; very weak. υ; stretching, δ; in plane bending: γ-out of plane bending

TABLE 3
EXPERIMENTAL WAVE NUMBERS OF Ag_2O (NANO LEVEL)

S. No.	Observed Frequency(cm^{-1})		Vibrational assignments
	FT-IR	FT-Raman	
1	780s	710s	(Ag-O)υ
2	750s	680s	(Ag-O)υ
3	640s	640s	(Ag-O)υ
4	580m	580w	(Ag-O)υ
5	490m	490s	(Ag-Ag)υ
6	470m	470w	(Ag-Ag)υ
7	310m	-	(O-Ag-O) δ
8	220w	220m	(O-Ag-O) δ
9	190w	190w	(O-Ag-O) γ
10	180w	180w	(O-Ag-O) γ
11	160w	-	(Ag-Ag) δ
12	120w	-	(Ag-Ag) γ

In the case of nano level of Ag_2O material, the Ag-O and Ag-Ag stretching modes were recognized at 780, 750, 640 & 580 cm^{-1} and 490 & 470 cm^{-1} respectively. The Ag-O and Ag-Ag in plane bending modes have been observed at 310 & 220 cm^{-1} and 160 cm^{-1} respectively. The Ag-O and Ag-Ag out of plane bending vibrational bands have been observed at 190 & 180 cm^{-1} and 120 cm^{-1} respectively.

Usually, the stretching bands of Ag-O and Ag-Ag for Ag_2O material are found in the region 520-675 cm^{-1} and 510-420 cm^{-1} [37-39] respectively. But, here, the bands of both cases observed in nano level were found to greater than macro level and the increment in wavenumbers was calculated to be 60-100 cm^{-1}. The in plane and out of plane vibrations were observed within the expected region and they were also elevated in the case of nano level. When the macro level material is reduced to the nano level, the surface area of the atoms will be increased much. Similarly, the force constant between the bonds also increased and thereby the vibrational frequencies related to the bonds will be shifted to the well beyond the expected region. So, all the vibrational bands were found at higher frequency level.

Apart from that, the vibrational region of the certain Ag-O and Ag-Ag bonds are moved up to the well above the allotted region of the spectrum which showed its activeness when compared with bonds which are located at some other places of the crystal. According to the present crystal lattice of FCC, the Ag-O and Ag-Ag bonds in (111), (200), (210), (220) and (311) planes were determined to be active. This result was supported by the observed data of XRD.

4. CONCLUSION

The Ag_2O nano material was fabricated using popular technique and in order to study its characteristics, the material was tested and evaluated making use of morphological, optical and electronic tools. The morphological data of the present compound emphasized the direct and reciprocal lattices and were FCC and BCC respectively. The lattice constants were calculated and the results of the same were validated by the experimental data. The surface effect was keenly observed from SEM images and it was validated by the TEM diagrams. The PL impact of present case was evaluate and the photo-emission characteristics were studied with the observed data. The UV-Visible recoded results were validated with the theoretical results and thereby opto-electronic character was examined. The SAED pattern was keenly observed and the results were discussed deeply and the fundamental pattern of the crystal lattice was predicted. The vibrational analysis was carried out and the activity of the compositional parts were assessed in the FCC associative planes.

REFERENCES

1. R.M. Crooks, M. Zhao, L. Sun, V. Chechik, L.K. Yeung, Acc. Chem. Res. 34 (2001) 181–190.
2. A.D. McFarland, R.P. Van Deeyne, Nano Lett. 3 (2003) 1057–1062.
3. S.G. Sudrik, N.K. Chaki, V.B. Chavan, S.P. Chavan, H.R. Sonowane, K. Vijayamohanam, Chem. Eur. J. 12 (2006) 859–864.
4. K. Yoosaf, B.I. Ipe, C.H. Suresh, K.G. Thomas, J. Phys. Chem. C 111 (2007) 12839–12847.

5. S. Sun, C.B. Murray, D. Weller, L. Folks, A. Moser, Science 287 (2000) 1989–1992.
6. L. Kwati, B. Ahmmad, H. Okamura, J. Kurawaki, Colloids Surf. B 82 (2011) 391–396.
7. S. Nie, S.R. Emory, Science 275, (1997) 1102–1106.
8. B.J. Sanghavi, A.K. Srivastava, Electrochim. Acta 55 (2010) 8638–8648.
9. B.J. Sanghavi, A.K. Srivastava, Electrochim. Acta 56 (2011) 4188–4196.
10. V.K. Gupta, A.K. Jain, G. Maheswari, Talanta 72 (2007) 1469–1473.
11. B. J. Murray, Q. Li, J. T. Newberg, E. J. Menke, J. C. Hemminger andR. M. Penner, Nano Lett., 2005, 5, 2319.
12. M. Bielmann, P. Schwaller, P. Ruffieux, O. Groning, L. Schlapbachand P. Groning, Phys. Rev. B: Condens. Matter Mater. Phys., 2002,65, 235431.
13. N. Yamamoto, S. Tonomura, T. Matsuoka and H. Tsubomura, Jpn.J. Appl. Phys., 1981, 20, 721.
14. B. J. Murray, Q. Li, J. T. Newberg, E. J. Menke, J. C. Hemminger andR. M. Penner, Chem. Mater., 2005, 17, 6611.
15. B. J. Murray, J. T. Newberg, E. C. Walter, Q. Li, J. C. Hemmingerand R. M. Penner, Anal. Chem., 2005, 77, 5205.
16. E. Tselepis and E. Fortin, J. Mater. Sci., 1986, 21, 985.
17. Y. Ida, S. Watase, T. Shinagawa, M. Watanabe, M. Chigane,M. Inaba, A. Tasaka and M. Izaki, Chem. Mater., 2008, 20, 1254.
18. B. E. Breyfogle, C. Hung, M. G. Shumsky and J. A. Switzer,J. Electrochem. Soc., 1996, 143, 2741.
19. Y. Her, Y. Lan, W. Hsu and S. Y. Tsai, J. Appl. Phys., 2004, 96, 1283.
20. J. Tominaga, J. Phys.: Condens. Matter, 2003, 15, R1101.
21. W. A. Parkhurst, S. Dallek and B. F. Larrick, J. Electrochem. Soc., 1984, 131, 1739
22. S. Dallek, W. A. West and B. F. Larrick, J. Electrochem. Soc., 1986, 133, 2451.
23. Junqing Pan, Yanzhi Sun, Zihao Wang, Pingyu Wan, Xiaoguang Liua and Maohong Fan, J. Mater. Chem., 2007, 17, 4820–4825.
24. P. Thiruramanathan, G.S. Hikku, R. Krishna Sharma, M. Siva Shakthi, Int. J. Techno Chem Res.,1(1), (2015) 59-65.
25. Chao Guo, Juan Xue, Yinsheng Dong, Materials Letters, Volume 219, 15, (2018), 182-185.
26. C. A. Yang, S. Yang, X. Liu, H. Nishikawa, C. R. Kao, Journal of Alloys and Compounds, Volume 762, 25, (2018) 586-597.
27. TaotaoLi, NingDang, Miaomiao Liang, ChunliGuo, HuihuLu, Jingyu Ma, WeiLiang, Applied Surface Science, 451, 1, (2018), 148-154.
28. J.B. Poole, Philips Tech. Runsch., 9, (1947), 33-39.
29. W. Kossel, G. Möllenstadt, Ann. der Phys., 36, (1939), 133-139.
30. M.J. Buerger, The precession method in X-ray crystallography. John Wiley and Sons, Inc. New York. 1964.
31. Samira Bagheri, Donya Ramimoghadam, Amin TermehYousefi, Sharifah Bee Abd Hamid, nt. J. Electrochem. Sci.,10 (2015), 3088 - 3097.
32. Kalyani Abhimanyu Kedar, Sanjay Ravindra Chaudhari, Avanapu Srinivasa Rao, Data in Brief, 17, (2018), 1188-1195.
33. Laura Galke, Christopher M. Stevenson, Journal of Archaeological Science: Reports, 2, (2015), 333-340.
34. S. Ashokkumar, S. Ravi, S. Velmurugan, Spectrochimica Acta Part A: Molecular and Biomolecular Spectroscopy 115 (2013) 388–392.
35. G. Rajakumar, A. Abdul Rahuman, Acta Trop. 118 (2011) 196–203.
36. Hayat Khan, Zhuoran Jiang, Dimitrios Berk, Solar Energy, 162, 1, (2018), 420-430.
37. S. Pal, Y.K. Tak, J.M. Song, Appl. Environ. Microbiol. 73 (2007) 1712.
38. A. K. Chawla, S. Singhal, H. O. Gupta, and R. Chandra,Thin Solid Films, 517, 3, (2008)1042–1046.
39. R. Swanepoel, Journal of Physics E, 16, 12,(1983) 1214.
40. J. Reichman, Handbook of Optical Filters for Fluorescence Microscopy (Chroma Technology, Brattleboro, 2010.
41. M. Niederberger, M. H. Bartl, and G. D. Stucky, Journal of the American Chemical Society, 124, 46, (2002), 13642–13643.
42. J. Y. Luo, F. L. Zhao, L. Gong et al. Applied Physics Letters, 91, 093124, (2007), 1-3.